DOI: 10.1002/ejic.200700284

Nb-Doped VO_2 Thin Films Prepared by Aerosol-Assisted Chemical Vapour Deposition

Clara Piccirillo,[a] Russell Binions,[a] and Ivan P. Parkin*[a]

Keywords: Intelligent materials / Vanadium dioxide (M) / Transition temperature / Niobium doping

Niobium-doped vanadium dioxide ($V_xNb_{1-x}O_2$, x = 0–0.037) thin films were prepared by aerosol-assisted chemical vapour deposition (AACVD) of vanadyl(IV) acetonate and niobium(V) ethoxide in ethanol. Samples were analysed by EDX, XRD, Raman, XPS and SEM. The analyses confirmed the deposition of niobium, even if no separated phase was formed; the morphological structure of the films was affected by the dopant presence. The thin films showed thermochromic behaviour, with a marked change in optical properties above and below the switching temperature.
(© Wiley-VCH Verlag GmbH & Co. KGaA, 69451 Weinheim, Germany, 2007)

Introduction

Vanadium(IV) oxide (VO_2) is a material with many interesting characteristics, including a thermochromic phase transition. At room temperature, the most stable phase is the monoclinic VO_2 (M); at higher temperature the rutile phase VO_2 (R) is stabilised. Above a certain temperature, there is a spontaneous transition from the monoclinic to the rutile form, a metal-to-semiconductor transition (MST), that is completely reversible and takes place at 68 °C.[1] A remarkable change in the physical properties is detected on passing through the MST transition; VO_2 (M) behaves as a semiconductor and does not reflect much solar energy, whereas VO_2 (R) is a semimetal and shows markedly higher electrical conductivity and a much higher reflectance, particularly in the infrared range.[2]

Vanadium dioxide represents an ideal material for use as an intelligent window coating, that is a coating that modifies its behaviour in response to an external stimulus, i.e. heat. The low reflectance of the monoclinic phase assures that a coated window allows maximum solar gain on cooler days (T below T_c). The transition to the rutile phase, on the other hand, can help to reduce the heat gain in hot days. The effect would be to have a comfortable environment with reduced air-conditioning costs, which has economical and environmental benefits.[2]

For practical application an intelligent window coating should have its phase-transition temperature closer to a comfortable room temperature value. It has been reported previously that a change in the transition temperature can be obtained by doping metal ions into the VO_2 lattice; doping with titanium, for instance, raises the value of T_c[3] while tungsten, molybdenum and niobium lower it.[4,5]

Up to now, the best reduction in the transition temperature has been obtained by the use of tungsten; in fact W-doped VO_2 thin films have been prepared with different methodologies such as sputtering,[6,7] sol-gel,[8] atmospheric-pressure and aerosol-assisted chemical vapour deposition (APCVD and AACVD).[2,9] These films show a decrease in the transition temperature that is proportional to the amount of tungsten incorporated; samples containing about 1% tungsten, show a decrease of 20–25 °C.[2,6,7] Considering in particular the AACVD methodology, films with values of T_c close to room temperature were deposited.[9]

Niobium-doped VO_2 thin films have been prepared by sol-gel[10] and APCVD methodologies.[5] The results seemed particularly encouraging for APCVD samples; in fact, above the transition temperature, they showed a remarkable decrease in the transmittance in the infrared region, fulfilling the requirement for intelligent window coatings. The problem, however, was the difficulty to incorporate large enough amounts of niobium into the VO_2 films, in fact the highest niobium concentration achieved was 0.4%, corresponding to a T_c value of 55 °C.[11]

In this paper we report the first synthesis of Nb-doped VO_2 thin films with AACVD. With this methodology the precursor is dissolved in a solvent and an aerosol generated ultrasonically. An inert carrier gas transports the precursor (within the aerosol droplets) to the deposition reactor where the reaction takes place. The main advantage of AACVD deposition is that, unlike for APCVD, the precursor does not need to be volatile but just soluble in a solvent appropriate for the aerosol formation.[12] In this way it is possible to use different precursors, not normally used in APCVD.[13,14] Previous work indicates a strong correlation between metal ratios in the precursor solution and those found in the resultant film.[9] AACVD provides an easy method to prepare multi-component and/or doped films.

[a] University College London, Chemistry Department, Christopher Ingold Laboratories,
20 Gordon Street, London, WC1H 0AJ, UK
E-mail: i.p.parkin@ucl.ac.uk

 InterScience © 2007 Wiley-VCH Verlag GmbH & Co. KGaA, Weinheim

Previous experiments were carried out by our group to deposit VO_2 (M) using AACVD methodology (Figure 1). The effect of different experimental parameters such as solvent, deposition temperature and gas-flow rate was studied and the deposition conditions were optimised to deposit VO_2(M) as the only phase and with no contamination.[15] The same experimental conditions were used to deposit Nb-doped VO_2, with $[Nb(OC_2H_5)_5]$ added as a niobium precursor. Depositions with different Nb/V ratios were performed; the deposited films were analysed to determine their composition, their structure and their behaviour as an intelligent window material.

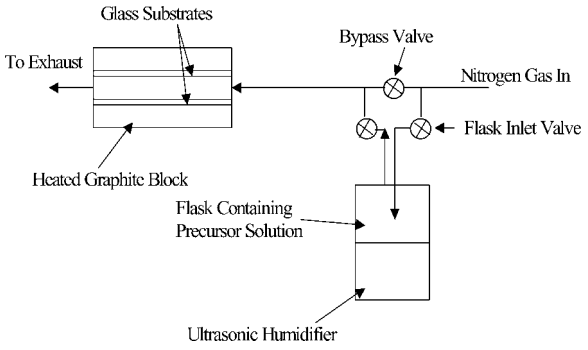

Figure 1. Schematic representation of AACVD experimental apparatus.

Results and Discussion

Film Deposition and Characterisation (Deposited Phases and Morphology)

Vanadium dioxide thin films with different amounts of niobium were deposited, by AACVD of a solution containing $[VO(acac)_2]$ and $[Nb(OEt)_5]$. Table 1 reports the Nb/V precursors ratio employed for the depositions. All deposited films were yellow in colour with some trace of brown, identical to undoped VO_2 films.[15] They all showed good adherence; they passed the Scotch tape test, but they could be scratched by a scalpel and were stable in air.

Table 1. Niobium/vanadium molar ratio for the initial solution and the deposited samples.

Sample	Nb/V solution molar ratio (%)	Nb/V film molar ratio (%)	$T_c \pm$ hysteresis width (°C)
1	1.3	0	58 ± 3
2	5.2	0	58 ± 3
3	7.5	2.6	42 ± 3.5
4	10.3	2.4	44 ± 3
5	12.4	2.2	35 ± 3
6	13.8	3.7	37 ± 3
7	14	3.0	35 ± 4
8	17	2.7	37 ± 3.5
9	18.9	2.8	41 ± 3

To determine the films' composition, i.e. the amount of niobium deposited in each film, EDX analyses were taken. The results are listed in Table 1. It can be seen that for precursor ratios in solution up to 5.2%, there is no niobium detected in the films. The reason for this behaviour is not clear, it is likely that the niobium precursor has to reach a critical concentration before it interacts with the vanadium; this would explain the sudden increase in the Nb/V film ratio from 0 to 2.6%.

For higher concentrations in solution, there is an increase of the niobium concentration in the deposits; however, the value reaches a plateau and it remains stable (within experimental error), despite the increase in concentration of niobium in solution. An explanation for these results can be that the value of the solubility limit on niobium in vanadium is reached; however, no data are available in literature to confirm this.

From this data it can be seen that niobium behaves very differently from tungsten in VO_2 films deposited by AACVD; in fact a linear correlation was observed for tungsten between the amounts of precursor in solution and the metal in the film.[9] Furthermore, a much greater proportion of the tungsten precursor was included in the VO_2 film as metal dopant (e.g. a W/V atom ratio of about 6% in solution corresponded to about 2% in the film).

The different behaviour of niobium confirms the difficulties previously reported with this metal already observed in APCVD.[11] In comparison a much greater amount of metal was deposited in the AACVD samples; this indicates the suitability of the technique for the deposition of multicomponent/doped films.

The XRD patterns of all samples were recorded to determine the nature of the phases present; Figure 2 shows the XRD spectrum of sample **5**. It can be seen, despite the glass background signal, that the deposited film is unambiguously VO_2(M).[2] Similarly to undoped VO_2 and W-doped VO_2 deposited by AACVD, no preferential orientation is observed.[9] No other phase was detected, neither for niobium nor for other vanadium oxides. Other areas of the same film showed the same pattern, indicating good homogeneity of the film. All the thin films investigated, with different niobium concentration, had the same characteristics; this indicates that the amount of dopant does not affect the nature of the phase deposited and that, under these conditions, it does not favour the formation of mixed phases.

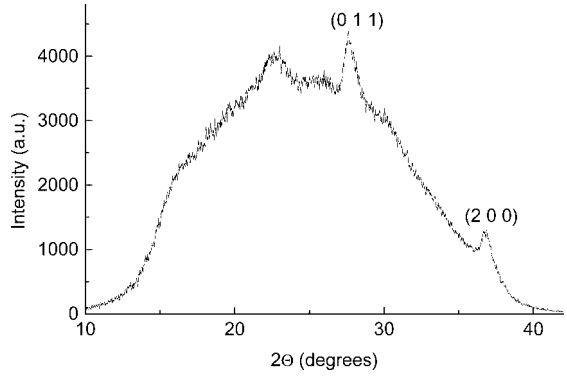

Figure 2. XRD spectrum of sample **5**.

 © 2007 Wiley-VCH Verlag GmbH & Co. KGaA, Weinheim

The Raman spectrum of sample **5** is shown in Figure 3. It can be seen that it shows the characteristics VO_2 pattern. In fact all the detected signals can be assigned to VO_2 (M); furthermore, there is no signal corresponding to graphitic carbon (i.e. at 1355 cm^{-1}), indicating no carbon contamination of the film.

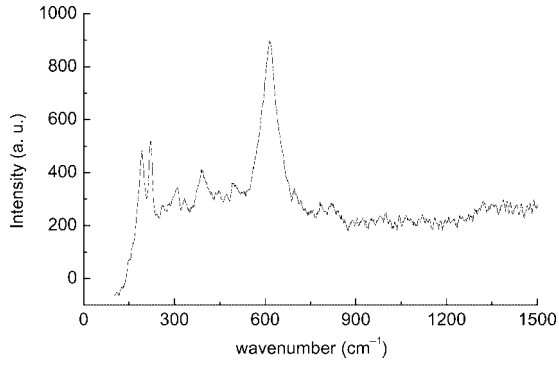

Figure 3. Raman spectrum for sample **5**.

XPS spectra of Nb-doped VO_2 samples were acquired to detect the possible other elements deposited in the film as impurities and to determine the oxidation states of the main film components. From the analysis of the survey spectrum (registered on the surface of the film), it was seen that the only additional element detected in the film is carbon. However, the intensity of the carbon signals decreased remarkably moving from the surface into the bulk of the film; this indicates the carbon is present only on the surface as contaminant from the external environment, but it is not present in the bulk of the film. This is in agreement with what was observed by Raman spectroscopy; in fact the signals in the Raman spectra are related to the bulk of a material and not just to its surface.

Figure 4(a) and (b) show the sections of the spectrum corresponding to the niobium and vanadium, respectively, for sample **5**; as mentioned above, the spectrum was registered on the surface of the film. The niobium peaks were detected for $Nb3d_{5/2}$ and $Nb3d_{3/2}$ at the binding energies of 207.0 and 209.2 eV. These values correspond to the binding energies of Nb_2O_5, therefore it follows that the niobium oxidation state is +5.[16] This is in agreement with previously published data,[11] hence it confirms that niobium does not change its oxidation state during the deposition. Spectra acquired in the bulk of the film show that niobium has the same oxidation state throughout the film.

The analysis of the part of the spectrum corresponding to vanadium shows that the main signal consists of two overlapping peaks at 516.2 and 517.4 eV (the deconvolution is shown in Figure 4). These two binding energies correspond to $V2p_{3/2}$ (+4) and $V2p_{3/2}$ (+5).[16] This indicates that, on the surface of the film, VO_2 is partly oxidised to V_2O_5.

Moving to the bulk of the film, however, only the peak corresponding to V^{IV} is detected (spectrum is not shown). These results are in agreement with the XRD and Raman results; in fact no V_2O_5 signal was observed by either technique (see Figures 2 and 3), because they analyse the bulk of the film and not just the surface.

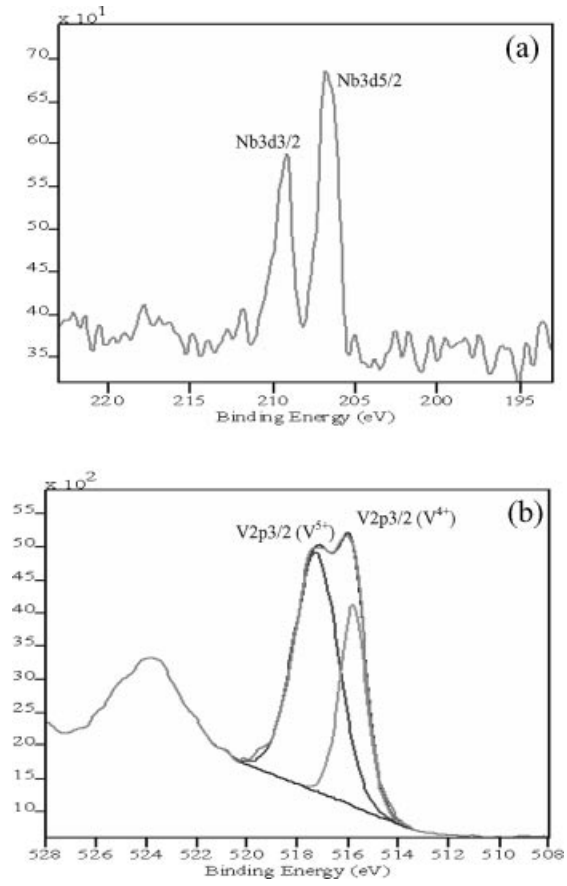

Figure 4. XPS spectrum for sample **5**: (a) niobium section; (b) vanadium section.

The morphology of the Nb-doped VO_2 thin films was studied by scanning electron microscopy (SEM). Figure 5 compares the surface structure of undoped VO_2 [Figure 5(a)] with the one of Nb-doped VO_2 [sample **7**, Fig-

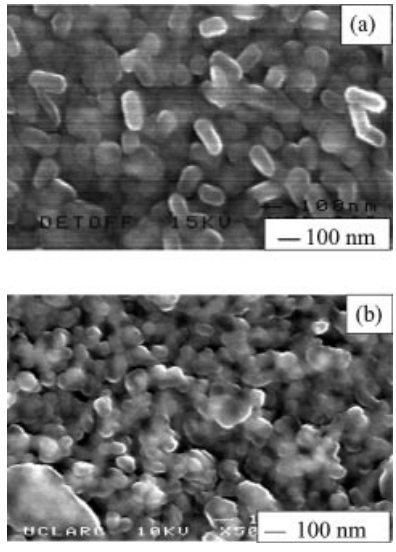

Figure 5. SEM images for (a) undoped VO_2; (b) sample **7**.

 © 2007 Wiley-VCH Verlag GmbH & Co. KGaA, Weinheim

ure 5(b)], both deposited using AACVD. It can be observed that they look quite different, indicating the effect of niobium on the film structure. Other films with different niobium concentrations have a similar morphology, indicating that the amount of niobium does not have any influence on the morphology.

Film Characterisation: Functional Properties

The optical properties of the samples were investigated and their thermochromic change through the monoclinic-rutile phase transition studied. The change in transmittance and reflectance above and below the transition temperature was measured to assess the efficiency and the suitability of this material as an intelligent window coating.

Figure 6 shows the transmittance and reflectance spectra above and below the transition temperature for sample **9**. Considering the transmittance [Figure 6(a)], there is a significant decrease above the transition temperature (up to 30%) in the infrared range. The spectra of all the other samples showed the same features, with some changes in the extent of the decrease in the transmittance, which was dependant on the thickness of the films. This behaviour is analogous to the one shown by both undoped and W-doped VO_2.[9,15]

The change in the reflectance, however, has different characteristics depending on the niobium content of the film; Figure 6(b) and (c) show the reflectance spectra of samples **5** and **9**, respectively. For sample **5**, an increase above T_c can be observed for the full infrared range; for sample **9**, on the contrary, such increase can be seen only for wavelengths larger than 1650 nm. At about 1650 nm the two lines cross over, therefore the curve corresponding to the reflectance above T_c is slightly less intense than the one representing the reflectance below T_c. Similar to the Raman spectra, this different behaviour was observed for samples **6**, **7**, **8** and **9**, when the niobium concentration in the films is about 3%; the two curves cross over in a range of energy between 1550 and 1650 nm. The comparison of these results suggests that probably the presence of another phase affects the change in the reflectance, limiting it to a smaller energy range.

The value of the transition temperature was also determined for each sample. This was done by measuring the transmittance at 4000 cm^{-1} as a function of the temperature. Figure 7 shows as an example the measurements for samples **4** and **7** (Nb/V = 2.4 and 3.0%, respectively). As shown in Figure 7, the transition temperature was determined considering the average value of the transmittance; the midpoint of the hysteresis loop for this value of transmittance is the transition temperature. It can be seen that the larger the Nb/V ratio, the lower is the value of the temperature. This shows the effectiveness of niobium to decrease T_c. Table 1 reports the value of T_c for every sample ± the width of the hysteresis loop. Similarly to what is observed for W-doped VO_2 deposited with AACVD, the width of the hysteresis loop does not change with the decrease of the transition temperature which is constant between 3 and 4 °C.

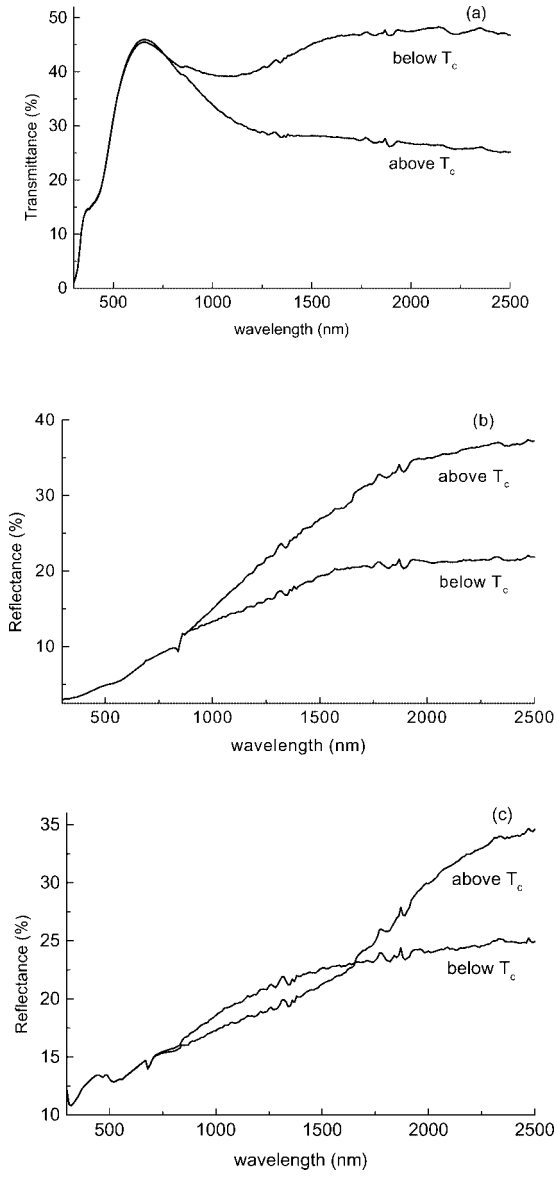

Figure 6. Optical properties above and below T_c. (a) Transmittance for sample **9**; (b) reflectance for sample **5**; (c) reflectance for sample **9**.

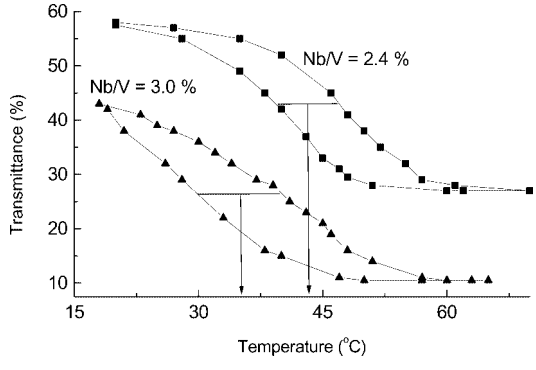

Figure 7. Transmittance at 4000 cm^{-1} as a function of the temperature for samples **4** and **7** (Nb/V atom ratio 2.4 and 3%, respectively).

 © 2007 Wiley-VCH Verlag GmbH & Co. KGaA, Weinheim

Figure 8 shows the value of T_c as a function of the niobium content in the film and that a good linear correlation is established. From this data it can be seen that an amount of niobium in the film of 2% lowers the transition temperature by 15 °C. It follows that niobium is less effective than tungsten to decrease the value of T_c (for tungsten, 1% of dopant decreases T_c by about 22 °C);[9] it is, however, still possible to achieve values of transition temperatures close to room temperature.

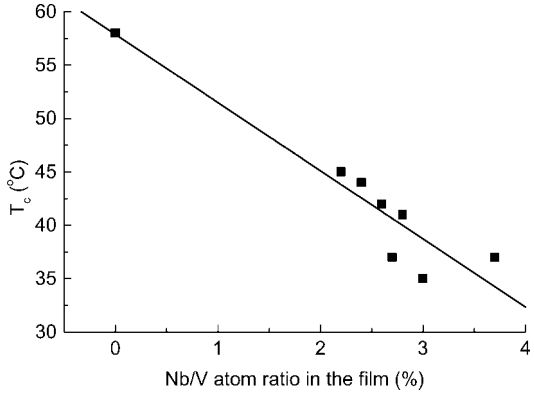

Figure 8. Transition temperature vs. the Nb/V atom ratio in the films.

Conclusions

Nb-doped VO_2 thin films were successfully deposited by *A*erosol-*A*ssisted *C*hemical *V*apour *D*eposition (AACVD). EDX analysis showed that an increase in the niobium concentration in solution correlates to an increase in niobium in the film as well, until a plateau is reached. Samples with a niobium content up to 3.7% (atom ratio) were prepared, VO_2 films with such high niobium concentrations were never deposited before. This indicates the suitability of the AACVD methodology to deposit doped thin films.

Films were characterised by several analytical techniques (XRD, Raman, SEM, XPS) to determine the nature of the deposited phase and to detect possible impurities. The functional properties of the films (reflectance/transmittance, transition temperature) were studied as well, to test their application as an intelligent material for window coating. Significant changes in the transmittance and reflectance properties were observed on passing the transition temperature; furthermore, a decrease in the transition temperature was observed, with a linear correlation, between the films' niobium content and the value of the temperature. These features indicate Nb-doped VO_2 as a suitable material for application in smart windows.

Experimental Section

Film Deposition: Vanadyl(IV) acetylacetonate $[VO(C_5H_8O_2)_2]$ = $[VO(acac)_2]$ and Nb^V ethoxide $[Nb(OC_2H_5)_5]$ were purchased from Aldrich Chemical Co and used as supplied. The aerosol solution was prepared by dissolving both precursors in ethanol. For $[VO(acac)_2]$, a constant concentration of 0.05 mol dm^{-3} was used. Different molar amounts of $[Nb(OC_2H_5)_5]$ were used, in order to have a varying Nb/V molar ratio (5.2–17 mol-%). An aerosol was generated from 50 mL of precursor solution using a Mountain Breeze humidifier; a nitrogen flow of 1.5 L min^{-1} (BOC, 99.9%) was passed through the aerosol mist, directing the aerosol to a horizontal bed cold wall CVD reactor. Sheets of float glass ($150 \times 45 \times 4$, Pilkington Glass Plc.) were used as deposition substrates; an SiO_2 layer, about 50 nm thick, was used to suppress the diffusion of ions from the bulk glass. Prior to the deposition, the substrates were cleaned using water, acetone and 2-propanol and then dried in air. A Tempatron TC4800 thermostat was used to heat the substrates, with the temperature monitored by a Pt-Rh thermocouple. The substrates were heated to a temperature of 500 °C. The aerosol passed between the heated substrate and a glass top plate, placed 8 mm above the substrate and parallel to it. The exhaust was vented into a fume cupboard. The gas flow was continued until all the precursor solution had passed through the reactor; it normally took between 40 and 50 min. At the end of the deposition, the nitrogen flow through the aerosol was diverted and only nitrogen passed over the substrate. A schematic representation of the AACVD deposition apparatus is shown in Figure 1.

Film Characterisation: X-ray powder diffraction patterns were measured with a Bruker D8 diffractometer using filtered (Cu-$K_{\alpha 1+\alpha 2}$) radiation in the reflection mode using glancing angle incidence (1.5°). SEM was carried out with a Hitachi filament scanning microscop. EDAX was determined with a Philips XL30 ESEM instrument, data was quantified using Oxford Inca Software. Raman measurements were carried out with a Renishaw system 1000 Raman spectrometer, with an Ar laser excitation source (514 nm). The Raman system was calibrated against the emission lines of argon. X-ray photoelectron spectroscopy (XPS) measurements were carried out with a VG ESCALAB 220i XL instrument using monochromatic Al-K_α radiation. Binding energies were referenced to surface elemental carbon at 284.6 eV. Depth profiling was carried out using a 3-kV argon ion gun operating at 0.5 μA to sputter the surface of the film. Reflectance and transmission spectra were recorded between 300 and 2500 nm with a Perkin–Elmer Lambda 950 UV/Vis spectrometer. Measurements were standardised relative to a Spectralon® standard (reflectance) and air (transmission). For measurements at different temperatures, an aluminium temperature cell, controlled by RS resistive heaters, Eurotherm temperature controllers and k-type thermocouples were used to manipulate the sample temperature. The sample temperature was measured using a k-type thermocouple taped directly onto the film surface.

Acknowledgments

This research was financially supported by the EU project Termoglaze COOP-CT-2005-017761. The authors would like to thank Pilkington Glass for providing the deposition substrates, Mr. Kevin Reeves for the help with scanning electron microscopy, Dr. Steve Firth for the help with Raman spectroscopy. I. P. P. thanks the Royal Society/Wolfson Trust for a merit award.

[1] F. J. Morin, *Phys. Rev. Lett.* **1959**, *3*, 34–36.
[2] T. D. Manning, I. P. Parkin, R. J. H. Clark, D. Sheel, M. E. Pemble, D. Vernadou, *J. Mater. Chem.* **2002**, *12*, 2936–2939.
[3] F. Beteille, R. Morineau, J. Livage, M. Nagano, *Mater. Res. Bull.* **1997**, *32*, 1109–1117.
[4] T. D. Manning, I. P. Parkin, M. E. Pemble, D. Sheel, D. Vernardou, *Chem. Mater.* **2004**, *16*, 744–749.

 © 2007 Wiley-VCH Verlag GmbH & Co. KGaA, Weinheim

[5] T. D. Manning, I. P. Parkin, C. Blackman, U. Qureshi, *J. Mater. Chem.* **2005**, *15*, 4560–4566.
[6] W. Burkhardt, T. Christmann, B. K. Meyer, W. Niessner, D. Schalch, A. Scharmann, *Thin Solid Films* **1999**, *345*, 229–235.
[7] P. Jin, S. Nakao, S. Tanemura, *Thin Solid Films* **1998**, *324*, 151–158.
[8] I. Takahashi, M. Hibino, T. Kudo, *Jpn. J. Appl. Phys.* **2001**, *40*, 1391–1395.
[9] C. Piccirillo, R. Binions, I. P. Parkin, *Thin Sol. Films*, submitted for publication.
[10] C. B. Greenberg, *Thin Solid Films* **1983**, *110*, 73–82.
[11] T. D. Manning, Ph. D. Thesis, London, **2004**.
[12] K. L. Choy, *Prog. Mater. Sci.* **2003**, *48*, 57–170.
[13] W. B. Cross, I. P. Parkin, *Chem. Commun.* **2003**, *14*, 1696–1697.
[14] R. Binions, C. J. Carmalt, I. P. Parkin, *Thin Solid Films* **2004**, *469–470*, 416–419.
[15] C. Piccirillo, I. P. Parkin, R. Binions, *Chem. Vap. Depos.*, in press.
[16] C. D. Wagner, A. V. Naumkin, A. Kraut-Vass, J. W. Allison, C. J. Powell, J. R. Rumble, *NIST X-ray Photoelectron Spectroscopy Database*, version 3.4 (web version), NIST, **2003**, http://srdata.nist.gov/xps/.

Received: March 12, 2007
Published Online: July 11, 2007

 © 2007 Wiley-VCH Verlag GmbH & Co. KGaA, Weinheim